JPE 9-4-11

Comparison of Various Methods to Mitigate the Flicker Level of DFIG in Considering the Effect of Grid Conditions

Yun-Seong Kim*, Aditya Marathe*, and Dong-Jun Won†

†*Dept. of Electrical and Electronics Eng., INHA University, Incheon, Korea

ABSTRACT

The short circuit ratio (SCR) of a given grid is able to show the stability of the system in the case of unwanted elements, such as wind turbulence. This paper presents the simulation of a model of the doubly fed induction generator in the simulation software PSCAD/EMTDC. This model has been used to study flicker during continuous operation and the effect of SCR and grid impedance angle on flicker emission. Simulation results show that compensation of the stator reactive power is an effective method to considerably reduce the flicker levels, irrespective of the grid conditions.

Keywords: Doubly fed induction generator, Flicker, reactive power control, Short circuit ratio, Variable speed, Wind turbine

1. Introduction

The continuously increasing need to generate electrical energy from renewable sources has thrown open the research of wind energy at full gear in many nations. Gaining more and more output power has been the primary aim of development of the wind turbine systems. The largest productions today are specified to deliver 1.5 - 2.5 MW output power [1]. With this increases in wind power penetration into the grid, the influence of wind turbines on the quality of power has become an important issue. Unwanted components such as wind turbulence and wind gusts, and grid conditions such as short circuit ratio and grid impedance angle, etc. lead to a flicker in the line voltages. This then leads to a flicker in the illumination caused by a simple light bulb, as perceived by the human eyes. Flicker thus causes irritation to the consumer at the receiving end [2].

The main focus of this paper is to study the integration of wind turbines into grids, especially weak grids. For this we will consider the effect of a) Short Circuit Ratio and b) Grid Impedance Angle, on flicker emissions.

In order to achieve such high power, the modern high-power turbines make use of adjustable speed generators (ASG). Simple pitch control, reduced mechanical stress, improved power quality and system efficiency, and reduced acoustic noise because of the ability to operate at low speeds, are the prime features of such generators [1]. The preferred topology to derive high power output from ASG is the Doubly Fed Induction Generator (DFIG). The DFIG is an implementation of the Scherbius Drive to control the induction machine. Using a

Manuscript received Dec. 22, 2008; revised May 30, 2009
†Corresponding Author: djwon@inha.ac.kr
Tel: +82-32-860-7404, Fax: +82-32-863-5822, INHA Univ
*Dept. of Electrical Engineering, INHA University, Korea

DFIG, the converters need only be rated to the rotor power, which is typically one-fourth of the rated system power. In comparison to a Kramer drive, the four-quadrant operation of the DFIG enables decoupled control of the active and reactive powers. The flicker emitted during operation of the DFIG is reduced by means of reactive power compensation. This can be achieved by using a STATCOM or by controlling the reactive power in the grid side converter.

The simulation software PSCAD/EMTDC [3], [4] has been used to develop a two megawatt level simulation model of the DFIG presented in this paper. This model has been used to study the effect of grid conditions on the flicker emitted by the DFIG.

2. Modeling the DFIG

The doubly fed induction generator has an AC-AC converter in the rotor circuit, popularly known as the Scherbius Drive. The power converter needs only to be rated to handle the rotor power which happens to be less than a quarter of the stator power. Vector control techniques are used to control the active and reactive powers in a decoupled manner. Most DFIG systems employ either a current fed DC link converter or cycloconverter. Both of them have certain disadvantages, which can be overcome by using two back-to-back PWM converters that are voltage fed and current-regulated [1]. Fig. 1 shows the schematic diagram of a doubly fed induction generator using two back-to-back PWM converters.

Modeling the DFIG involves modeling of the wound rotor induction machine, the rotor side converter, the grid side converter and the back-to-back PWM converters with the DC link between them, along with the aerodynamic model of the wind turbine. In this paper, vector controlled models of the rotor side and the grid side controllers are developed [5], [6]. For the wound rotor induction machine, the elaborate model from the simulation software PSCAD/EMTDC library is used. For the converters, standard electrical components models are used from the PSCAD/EMTDC library. The aerodynamic model of the wind turbine and the model of the wind profile are built with custom components made in PSCAD/EMTDC.

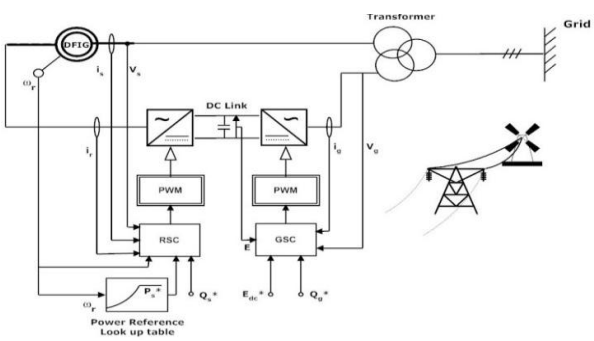

Fig. 1. Doubly Fed Induction Generator.

2.1 Wind Turbine Model

The aim of this paper is to study the effect of grid conditions on the electrical behaviors of the system, so the mechanical systems are simplified to some extent. The aerodynamic model of the wind turbine [6] is based on the following equation which gives the relation between the wind speed and the mechanical power captured by the turbine:

$$P_{mech} = \frac{1}{2} C_p \rho \pi r^2 v^3 \quad (1)$$

It depends on power coefficient C_p given for wind velocity v. C_p is generally defined as a function of the tip speed ratio λ and the pitch angle β.

$$\lambda = \frac{\omega r}{v} \quad (2)$$

where ω is the rotational speed of the turbine, and r is the radius of the rotor. The wind turbine model used in this study takes the wind profile as input and generates an output mechanical power and torque. This mechanical power is set as the reference for the stator real power output. The wind source model has been used from the PSCAD/EMTDC library, and it provides settings for mean wind speed, gust, ramp and noise components. When the wind speed crosses the rated wind speed for the generator the power reference sets to 1.0 p.u. This generates the maximum rated power in case of high wind speeds.

2.2 Reference Frames

When simulating the DFIG, we must note that the

voltages and currents measured are in the respective natural reference frames of the stator and the rotor. For the stator, the natural reference frame is the stationary frame oriented with the stator voltage. For the rotor, it is the frame rotating at the speed of the rotor. In order to control the system, we need to bring all quantities to a common reference frame. In order to change the reference frame, two basic transformations are involved. 1) The Clarke's Transformation: used to transform quantities from a three phase to a two phase system. 2) The Park's Transformation: used to rotate the two-axis system around any angle (see Appendix A). This is similar to vector rotation. In order to transform back from a rotating frame to the stationary frame, the inverse Park's transformation is used. Similarly, to get back the three phase system from the two phase system, the inverse the Clarke's Transformation is used.

For the rotor side controller, the preferred frame of reference is a synchronously rotating two-axis frame attached to the stator flux vector. Since we are connecting the machine to a grid, the stator flux remains more or less constant [1].

2.3 Rotor Side Controller (RSC)

The rotor side controller controls the induction machine. Selecting the synchronously rotating reference frame attached to the stator flux vector allows decoupled control of the electrical torque and rotor excitation current. Thereby we can control the stator active and reactive powers, and hence the power factor. Since the stator is connected to the grid, and the influence of the stator resistance is small, the stator magnetizing current i_{ms} can be considered constant. The stator flux angle is calculated as follows [5], [7]:

$$\psi^{s}{}_{s\alpha} = -\int (V^{s}{}_{s\alpha} - R_s i^{s}{}_{s\alpha})dt \tag{3}$$

$$\psi^{s}s\beta = \int (V^{s}{}_{s\beta} - R_s i^{s}{}_{s\beta})dt \tag{4}$$

$$(\psi^{s}{}_{s\alpha}, \psi^{s}{}_{s\beta}) \rightarrow (\psi^{s}{}_{s}, \theta_s) \tag{5}$$

$$\frac{\psi^{s}{}_{s\alpha}}{L_0} = i_{ms} \tag{6}$$

This flux is fed to a filter to remove any DC offset that may be present [7].

To achieve control of the active and reactive powers flowing out of the generator's stator, two cascades of two PI controllers are each used. The generated active and reactive powers are compared with the reference values and the errors are used to get the reference currents for the rotor. These are then compared to the actual rotor currents and the errors are used to generate the voltages to be applied to the rotor terminals. The following decoupling factors are added to these generated voltages [5], [6].

$$V_{dec,rd} = -\omega_{slip}\sigma L_r i_{rq} \tag{7}$$

$$V_{dec,rq} = \omega_{slip}(L_m i_{ms} \sigma L_r i_{rd}) \tag{8}$$

$$\sigma = 1 - \frac{L_m}{L_r} \tag{9}$$

The remaining scheme of the rotor side controller is as shown in fig. 2.

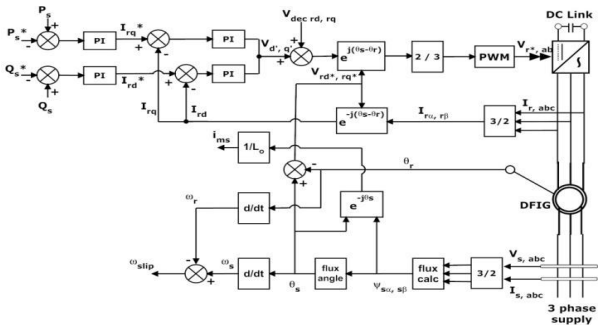

Fig. 2. Rotor Side Controller.

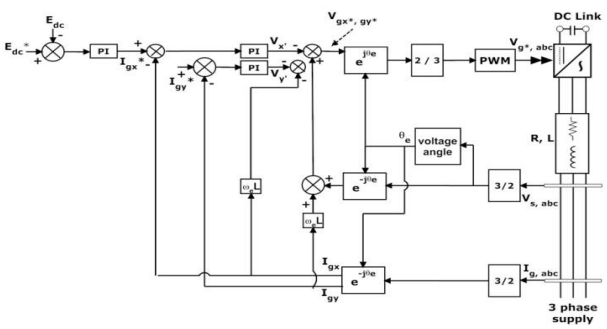

Fig. 3. Grid Side Controller.

2.4 Grid side Controller (GSC)

The objective of the grid side controller is to control the DC link voltage, which must be kept constant at all time. Independent control of the active and reactive power flowing through the grid side controller is done by using a reference frame oriented along the stator voltage vector. Fig. 3 shows the scheme of the grid side controller.

The DC link voltage is calculated from the DC power, which is the difference between the power flowing between the grid and the converter (P_g) and the power flowing in the rotor (P_r). The equation used in [5], [6], and [8] is as follows:

$$C\frac{dE_{dc}}{dt} = i_{os} - i_{or} = \frac{P_g}{E_{dc}} - \frac{P_r}{E_{dc}} \tag{10}$$

The error in the DC link voltage is used to generate the reference value for the d-axis current drawn by the grid side controller from the grid, and the reference for the q-axis current is set to zero to maintain the unity power factor. The real values of the currents are matched with these reference values by PI controllers. The PI controllers generate voltage reference values, which is addition to the decoupling factors are fed to the PWM converter on the grid side. The decoupling factors for the grid side controller are given by:

$$V_{dec,gx} = V_{sx} + i_q yL\omega_e \tag{11}$$

$$V_{dec,gy} = i_g xL\omega_e \tag{12}$$

The grid side PWM converter is modeled with a resistance and inductance so that we can control the current through the grid side controller if we know the voltages across the additional impedance [5], [6].

2.5 PWM Converter

In this study, the key focus is studying the flicker emission from the DFIG, and not the DFIG itself. To reduce the complexity involved with the modeling of the DFIG, the full scale PWM converters model is not used. Instead an average model using reference voltages and external impedance is used. Given the voltages across the impedance, we get the current through the converter. By controlling the reference voltage at one of the terminals, it is possible to control the currents, and hence any parameter in the grid side or the rotor side controller can be controlled [5].

3. Study System

The system simulated in this study is demonstrated in fig. 1 for the DFIG and fig. 2 and fig. 3 for the rotor side and the grid side controllers respectively. The entire wind turbine system is connected to a grid represented by an ideal voltage source and its Thevenin's equivalent impedance. The wind turbine drives a 2 MW doubly fed induction generator with back-to-back PWM converters connected in the rotor circuit.

For the rated wind speed and above the rated wind speed conditions, the wind turbine feeds a 2 MW mechanical power to the induction machine which is set as its reference for the stator active power. For conditions of wind speed below the rated speed, the full mechanical power absorbed by the wind turbine is fed to the induction machine as a reference for stator active power. The stator reactive power is always set to zero to maintain a constant unity power factor. The rated wind speed is set at 12 m/s.

The generator parameters are given in detail in the appendix.

4. Flicker

4.1 Flicker in a Power System

Wind turbines that are connected to the grid may produce a flicker during their normal course of operation. Flicker is defined as "an impression of unsteadiness of visual sensation induced by a light stimulus, whose luminance or spectral distribution fluctuates with time" [2]. In general, the visible flicker leads to human irritation. In places where the grids are weak or the wind penetration levels are high, a flicker can limit the integration of wind turbines. Fluctuations in the output power are caused by variations in the wind vector. Voltage fluctuations caused by load flow changes induce a flicker. Also, grid conditions such as the short circuit ratio of the grid and the grid impedance angle, and the type of wind turbine system used have an effect on the flicker levels. The doubly fed induction generator-based variable speed wind turbines

produce amongst the lowest of flicker levels [2]. Because of these and many other various reasons, there is a large scale integration of such wind turbine systems today. Therefore a study of flicker emission from a DFIG is very important.

4.2 Studying the Flicker in DFIG

In this paper, the effect of grid conditions (a) *SCR* and (b) grid impedance angle on a flicker in the line voltage is studied. Based on the model of DFIG developed in the simulation software PSCAD/EMTDC, the flicker emission of variable speed wind turbines during continuous operation is investigated. Out of the many factors that affect a flicker, the effect of grid conditions such as the short circuit ratio and the grid impedance angle are analyzed. The mitigation of flicker levels can be realized using output reactive power control or a STATCOM. The results for weak grids for different methods of flicker mitigation are hence analyzed and presented.

The voltage change across a power line is approximately calculated with the following formula [2]:

$$\delta V = \frac{PR_{th} + QX_{th}}{V} \tag{13}$$

where P and Q are the active and reactive powers flowing on the line and R_{th} and X_{th} are the resistance and reactance of the grid line. V is the terminal line voltage. This formula gives us the instantaneous change in the voltage level. Instantaneous changes in voltage level are studied on the basis of the change in luminous intensity perceived by the human eye. The IEC standard IEC 61 000-4-15 [2], [9], [10] describes a comprehensive model of a flicker meter. This model has been used to quantify the visible flicker in terms of numbers. It scales and filters the input voltage and then simulates the lamp-eye-brain response chain. On-line statistical analysis of the flicker signal then follows.

For our study, however, simplifications have been used. The line voltage flicker phenomenon is studied purely statistically. It gives similar, though not the same results, as the flicker meter model that studies the human eye-brain response to flicker. With this change in mind, the short term voltage flicker intensity has been termed as E_{st}. For the statistical analysis of the voltage levels themselves, the same equations those are used in the flicker meter model [2], [9], [10] have been adopted to calculate P_{st}:

$$E_{st} = \sqrt{A + B} \tag{14}$$

where

$$A = 0.0314E_{0.1}$$

and

$$B = 0.0525E_{1s} + 0.0657E_{3s} + 0.28E_{10s} + 0.08E_{50s}$$

The calculation is based on percentile values, $E_{0.1}$, E_{1s}, E_{3s}, E_{10s}, and E_{50s}. These values represent the voltage levels exceeded for 0.1, 1, 3, 10 and 50% of the time during the observation period. Just like in the calculation of P_{st}, the suffix s used in the equation (14) and (15) indicates that the smoothed values should be used:

$$\begin{aligned} E_{50s} &= \frac{(E_{30} + E_{50} + E_{80})}{3} \\ E_{10s} &= \frac{(E_6 + E_8 + E_{10} + E_{13} + E_{17})}{5} \\ E_{3s} &= \frac{(E_{2.2} + E_3 + E_4)}{3} \\ E_{1s} &= \frac{(E_{0.7} + E_1 + E_{1.5})}{3} \end{aligned} \tag{15}$$

Using these equations to analyze the flicker emission, we study the model for a flicker at different values of *SCR* and grid impedance angle.

The short circuit ratio and grid impedance angles [2] are defined as:

$$\begin{aligned} SCR &= \frac{S_k}{S_n} \\ \psi_k &= \arctan\left(\frac{X_{th}}{R_{th}}\right) \end{aligned} \tag{16}$$

where S_k is the short circuit apparent power of the grid and S_n is the rated apparent power of the wind turbines. R_{th} and X_{th} are the resistance and reactance of the grid respectively. In the next section we present the analysis of a flicker from a DFIG based wind turbine system, for different grid conditions as described above.

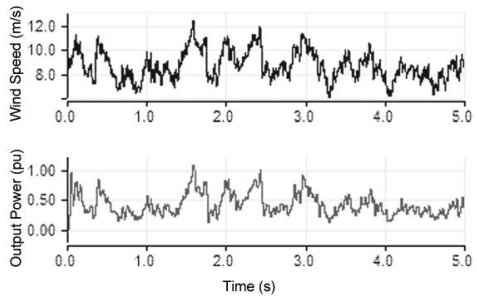

Fig. 4. Wind profile and corresponding output power of the wind turbine in the base case.

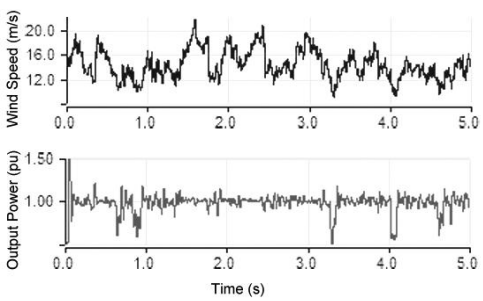

Fig. 5. Wind profile and corresponding output power of the wind turbine in the base case, but mean wind speed changed to 15 m/s.

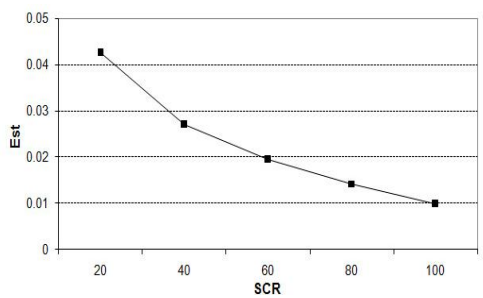

(a) High *SCR*

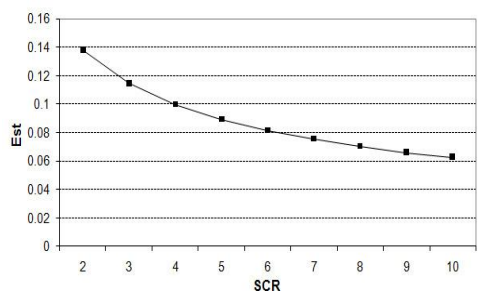

(b) Low *SCR*

Fig. 6. Variation of short term voltage flicker severity E_{st} with short circuit ratio. (ψ_k = 60°, v = 9 m/s)

5. Analysis

Flicker emissions of grid connected wind turbines depend on many factors such as wind parameters, grid connections, etc. We carry out the analysis of the flicker emissions for the following cases:

- Moderate to High *SCR* (Strong grids)
- Low *SCR* (Weak grids)
- Grid Impedance Angle

The base case for the simulation is the one with *SCR* = 20, ψ_k = 60 and wind speed 9 m/s. The base case means a normal setting for the simulation. Fig. 4 and 5 show the output power of the DFIG for wind below the rated speed (9 m/s) and above the rated speed (15 m/s) respectively. When the wind speed is low, the output power profile follows the wind profile. So the fluctuations are high. When the wind speed goes beyond the rated speed, pitch control takes over. At greater than the rated speed, the DFIG always generates rated power.

5.1 Moderate to High *SCR*

A grid having a *SCR* greater than 10 is supposed to be a strong grid, whereas a grid with *SCR* around 100 or more is a very strong grid. Fig. 6-(a) shows the variation of the voltage flicker levels with high *SCR* values, with a wind speed of 9 m/s. As the *SCR* increases, the grid becomes stronger. At higher *SCR*, the flicker levels are very small. As the grid strength increases the flicker levels fall appreciably.

5.2 Low *SCR*

A grid having a *SCR* of less than 10 is a weak grid. The flicker levels rise sharply as the *SCR* value falls below 10. Thus analysis of flicker emissions becomes very important for weak grids. Fig. 6-(b) shows the variation of the voltage flicker levels with low *SCR* values, for a wind speed of 9 m/s. The study and mitigation of flicker emission from the *DFIG* becomes very crucial at low *SCR* values.

5.3 Grid Impedance Angle

The power factor in the model is set to unity, and Fig. 7 gives a direct relation between the short term voltage flicker severity and the grid impedance angle. Equation

(13) can also be written as [2]:

$$\delta V = \frac{PR_{th}\cos(\psi - \psi_k)}{V\cos(\psi)\cdot\cos(\psi_k)} \quad (17)$$

According to the above equation, the voltage flicker levels are directly proportional to the difference between the power factor angle (ψ) and the grid impedance angle (ψ_k). As the difference between the two tends to be 90°, the voltage flicker tends to be zero.

6. Suggestive Analysis

Using some simple methods, the flicker levels can be greatly reduced. Reducing the flicker levels is an especially important task for integration of wind turbine systems with weak grids. According to equation 13, it is clear that some kind of reactive power compensation is needed which would cancel with the active power term and thereby reduce the flicker. Reactive power can be supplied by capacitor banks or a static compensator. A reactive power reference other than zero can also be set up in the rotor side controller of the DFIG and thus the flicker levels can be reduced. Furthermore, a reactive power controller can be used in the rotor side controller, but in that case it would mean that the machine would operate at a varying power factor. To bring this changing power factor to a constant value, external capacitor banks or other means may be used. We studied a few techniques to reduce the flicker levels and obtained the following results.

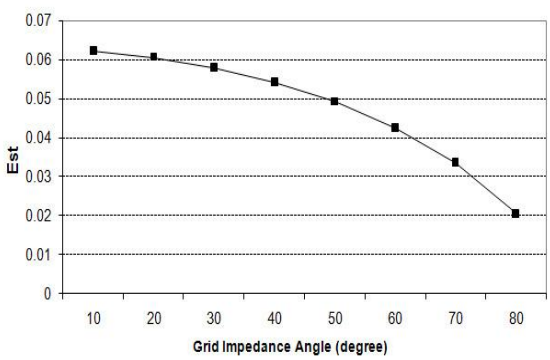

Fig. 7. Variation of short term voltage flicker severity E_{st} with grid impedance angle ψ_k. (SCR = 20, v = 9 m/s)

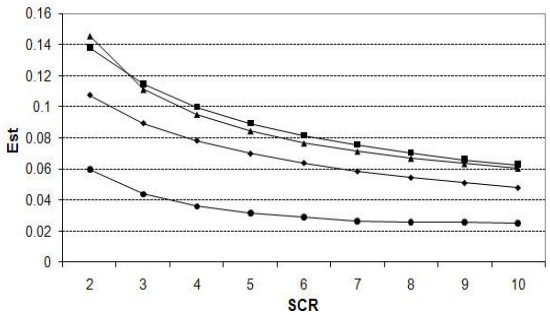

Fig. 8. Variation of short term voltage flicker severity E_{st} with SCR, reactive power set to: zero (square), 0.1 p.u. (diamond), 0.3 p.u. (circle), 0.5 p.u. (triangle). (ψ_k=60°, v = 9 m/s)

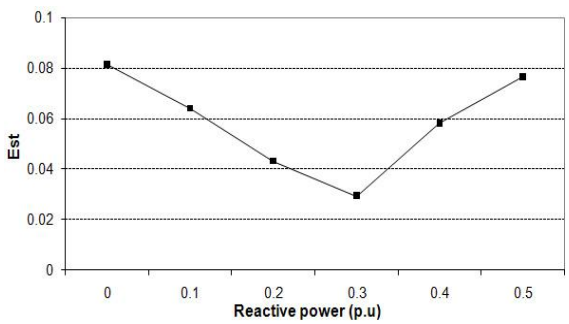

Fig. 9. Variation of short term voltage flicker severity E_{st} with Q_s injection. (SCR = 6, v = 9 m/s)

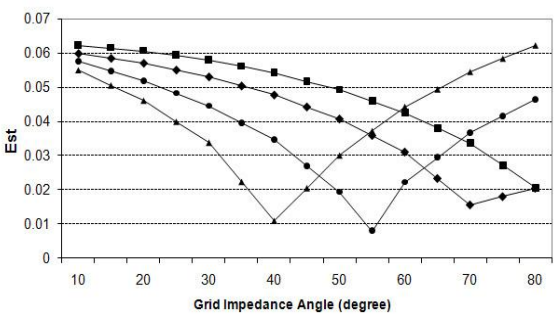

Fig. 10. Variation of short term voltage flicker severity E_{st} with grid impedance angle ψ_k, reactive power set to: zero (square), 0.1 p.u. (diamond), 0.3 p.u. (circle), 0.5 p.u. (triangle). (SCR = 20, v = 9 m/s)

6.1 Compensation by Reactive Power Control

In the original DFIG model, the reactive power reference was set to zero p.u. This was changed to 0.5 p.u. and the following results were obtained. It follows that if a reactive power is injected into the system, the flicker levels could be reduced considerably. This is evident from

fig. 8. Fig. 9 shows the variation of flicker levels with a change in the reactive power set point and the *SCR* fixed at 6. The flicker levels are reduced from a reactive power reference of 0.1 p.u. to 0.3 p.u., which then rise again.

Therefore, the limit value for flicker mitigation is achieved at 0.3 p.u. If a reactive power greater than 0.3 p.u. is injected, it gives rise to a negative voltage variation. The compensation by stator reactive power below the limit value can be efficient for flicker mitigation at weak grid conditions.

Fig. 10 shows the variation of flicker levels with grid impedance angle. When the grid impedance angle increases, a proper reactive power injection gives better performance than normal operation (set to zero).

Equation 17 explains that when the difference between the grid impedance angle (ψ_k) and the power factor angle (ψ) tends to be 90 degrees, the voltage flicker level is minimized. When the reactive power reference is set to zero, the power factor angle is zero and hence the flicker is minimized when the grid impedance angle tends to be 90 degrees. For minimum flicker, (ψ - ψ_k) must be 90 degrees and hence for different reactive power reference settings, the minimum flicker is achieved at different grid impedance angles. At 0.1 p.u. the minimum flicker is obtained around ψ_k of 70°, at 0.3 p.u. it is around ψ_k of 55° and at 0.5 p.u. around ψ_k of 40°.

By using the stator reactive power injection, appreciable flicker mitigation is observed. However, since the reactive power is fixed and active power is variable, the power factor is not constant. This needs to be corrected using additional components or control schemes.

6.2 Compensation by STATCOM

A Static Compensator (STATCOM) is a device that is capable of producing or absorbing reactive power using a combination of capacitors, reactors and power electronic switches. We have analyzed the flicker output of the DFIG on connecting to a STATCOM to the network. The PSCAD/EMTDC examples library provides a simple model of a 6 pulse voltage controlled PWM based STATCOM. We connected the STATCOM model to our wind turbine model to analyze the flicker levels. Fig. 12 shows the variation of flicker levels with *SCR* for weak grids. The STATCOM provides a good amount of flicker mitigation, but compared to the reactive power control method described in the previous section, the reduction is smaller for the low *SCR*.

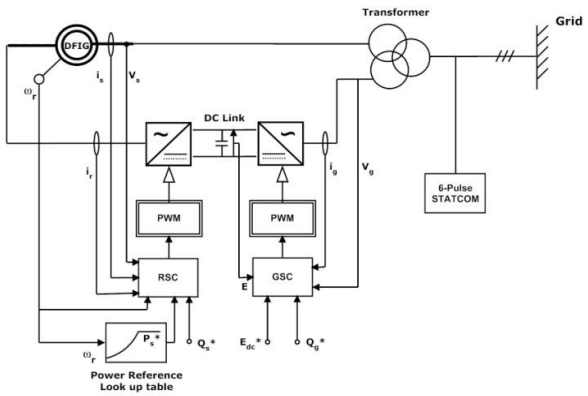

Fig. 11. Schematic diagram of the wind turbine system with STATCOM connected.

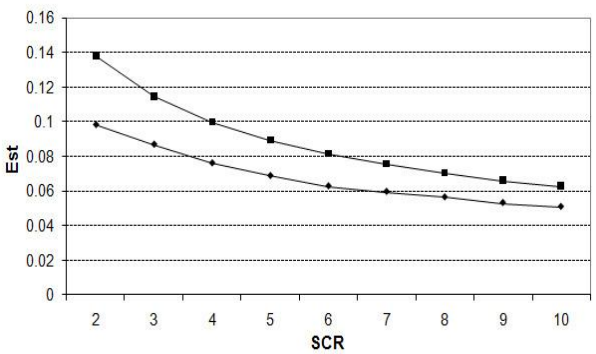

Fig. 12. Variation of short term voltage flicker severity E_{st} with *SCR*, STATCOM OFF (square), STATCOM ON (diamond). (ψ_k = 60°, v = 9 m/s)

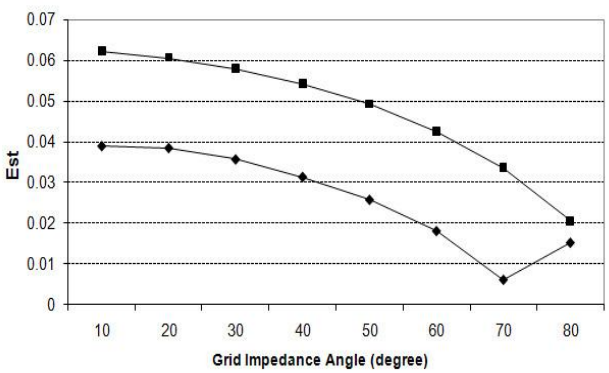

Fig. 13. Variation of short term voltage flicker severity E_{st} with grid impedance angle ψ_k, STATCOM OFF (square), STATCOM ON (diamond). (*SCR* = 20, v = 9 m/s)

Fig. 13 shows the variation of a flicker with a grid impedance angle. For grids that are very weak and also have a small grid impedance angle, the STATCOM provides an appreciable reduction of flicker levels. When the grid impedance angle approaches 70 degrees, it has a minimum flicker level. Since the absorption or generation of reactive power varies the power factor for a voltage, the grid impedance angle is varied at the time of the minimum flicker level.

Thus, the STATCOM is an efficient device for flicker mitigation. However, because the PWM switching inverter model is used for simulation, the flicker mitigation is prevented from switching in transient, which occurs from the dynamic characteristic of switching. We can effectively use the STATCOM to reduce flicker levels for weak grids.

6.3 Compensation by Voltage Control in the Rotor Side Controller (RSC)

Fig. 14 shows the voltage control scheme to reduce a flicker. In this scheme, a voltage at the point of common coupling (PCC) is maintained as a constant value (in this case voltage reference value is set at 1 p.u.). The voltage control produces Q_s^*, which is the reactive power reference value at the stator of the DFIG and regulates the voltage at the PCC.

In this study reactive power limits are set to ±2 p.u. Fig. 15 shows the variation of flicker levels with *SCR* for a weak grid. As can be seen, E_{st} has a low constant value during weak grid conditions. Compared to the methods of compensation by reactive power control and STATCOM discussed in previous sections, a direct voltage control scheme at the PCC provides the best performance for flicker mitigation. Fig. 16 shows the variation of flicker levels with grid impedance.

6.4 Comparison of various mitigation methods

The results show that the compensation by stator reactive power reference at 0.3 p.u. and the voltage control scheme have better performance for the flicker mitigation during low *SCR*. If the stator reactive power is set beyond limit, it has a reverse effect of increasing the flicker. This is proved from previous section 6.1. The voltage control and the STATCOM methods are effective for flicker mitigation because operation schemes are varied automatically by grid conditions. The STATCOM is implemented as absorbing or producing Q at the PCC with the grid line as parallel. The voltage control scheme adjusts the Q_s directly to reduce voltage flicker. It is shown that the series Q control is more effective than the parallel Q control. Fig. 18 shows the variation of flicker levels with grid impedance. Around a grid angle of 55 degrees the compensation by stator Q at 0.3 p.u. is more effective, and around 70 degrees the compensation by the STATCOM is more effective. However, on an overall average, the voltage control scheme is the most effective method to reduce flicker except at the grid impedance angles near 55 and 70 degrees.

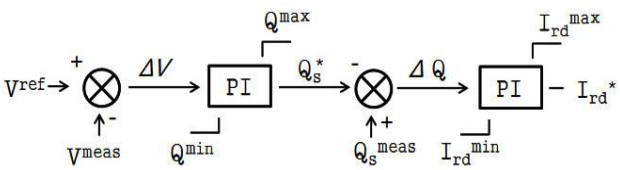

Fig. 14. Block diagram for voltage control through RSC.

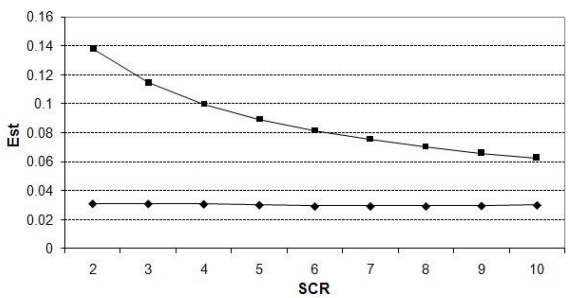

Fig. 15. Variation of short term voltage flicker severity E_{st} with *SCR*, reactive power set to zero (square), voltage control mode (diamond). (ψ_k = 60°, v = 9 m/s)

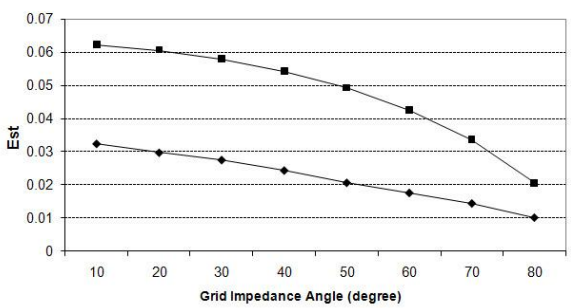

Fig. 16. Variation of short term voltage flicker severity E_{st} with grid impedance angle ψ_k, reactive power set to zero (square), voltage control mode (diamond). (*SCR* = 20, v = 9 m/s)

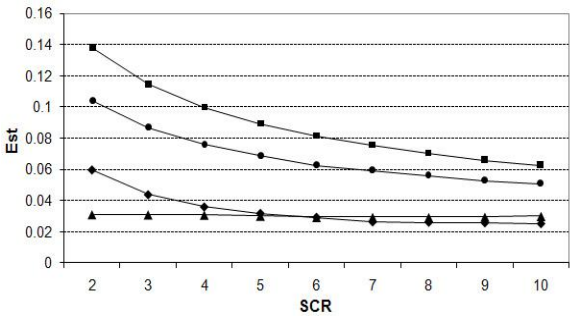

Fig. 17. Variation of short term voltage flicker severity E_{st} with *SCR*, reactive power set to zero (square), 0.3 p.u.(diamond), STATCOM ON (circle), voltage control mode (triangle). (ψ_k = 60°, v = 9 m/s)

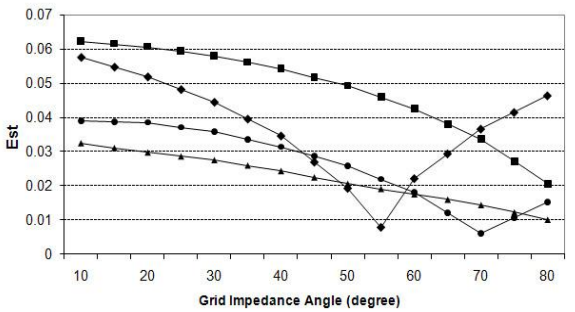

Fig. 18. Variation of short term voltage flicker severity E_{st} with grid impedance angle ψ_k reactive power set to zero (square), reactive power reference set to 0.3 p.u.(diamond), STATCOM ON (circle), voltage control mode (triangle). (*SCR* = 20, v = 9 m/s)

7. Conclusion

A model of a variable speed wind turbine with a doubly fed induction generator using back to back PWM voltage source inverters has been described in this paper. The flicker emission of the DFIG during continuous operation has been investigated using the developed model. From the simulation results it can be seen that grid conditions such as the short circuit ratio and the grid impedance angle significantly affect the level of voltage flicker. The levels of flicker emission rise steeply as the *SCR* falls into the weak zone.

The variable speed wind turbine with DFIG is made to control the output active and reactive power separately in a decoupled manner. It is concluded that reactive power compensation, which may be achieved by setting a reactive power reference greater than zero, or by using STATCOM, or voltage control at the rotor side converter, provides a simple way to control and mitigate the flicker emission levels in a DFIG. However, if active control of reactive power is done, then alternate ways to keep the grid power factor constant would have to be implemented.

Appendix

1. Clarke's Transformations

$$C = \begin{pmatrix} \frac{2}{3} & \frac{1}{3} & \frac{-1}{3} \\ 0 & \frac{\sqrt{3}}{3} & \frac{-\sqrt{3}}{3} \end{pmatrix}$$

2. Park's Transformation

$$C = \begin{pmatrix} \cos\theta & \sin\theta \\ -\sin\theta & \cos\theta \end{pmatrix}$$

3-1. Nomenclature

P_{mech} = Mechanical power captured by the wind turbine

P_s, Q_s = Active, reactive stator power

P_g = Active power flowing into grid side controller

P_r = Active rotor power

3-2. Voltages

V_r, V_s= Rotor, stator voltage

V_g = Grid side controller reference voltage

V_{dec} = Decoupling voltage

E_{dc} = DC link voltage

3-3. Currents

I_r, I_s= Rotor, stator current

I_g = Grid side controller current

i_{ms} = Stator magnetising current

i_{or} , i_{os} = Rotor-side, stator-side converter DC-link currents

ψ_s = Stator flux linkage

3-4. Machine parameters

L_m, L_r, L_s, L_0 = Machine inductances per phase

R_r, R_s = Machine resistances per phase

L, R= Grid side controller impedances per phase

θ_r,\ θ_s, \ θ_e = Rotor, stator flux vector, supply voltage position

ω_r, \ ω_e = Rotor, supply angular frequency

3-5. Wind Turbine

ρ = Air density

V = Wind speed

C_p= Power co-efficient
r = Rotor radius
3-6. Subscripts
a, b, c = Three phase, natural frame
α, β = Two axis, natural frame
d, q = Two axis frame, along stator flux vector
x, y = Two axis frame, along stator voltage vector

4-1. DFIG parameters
Rated power = 2 MW
Rated voltage = 0.69 kV
Base angular frequency = 366.99 rad/s
Angular moment of inertia = 0.5 p.u.
Mechanical damping = 0.01 p.u.
Stator resistance = 0.005 p.u.
Rotor resistance = 0.006 p.u.
Stator leakage inductance = 0.1 p.u.
Rotor leakage inductance = 0.1 p.u.
Mutual inductance = 3.3 p.u.

Acknowledgment

This work has been supported by KESRI (R-2007-1-015-01), which is funded by MKE (Ministry Knowledge Economy).

References

[1] S. Muller, M. Deicke, and R. W. De Doncker, "Doubly fed induction generator systems for wind turbines: A viable alternative to adjust speed over a wide range at minimal cost," *IEEE Ind. Appl. Mag.*, pp. 26-33, May/June 2002.
[2] T. Sun, Z. Chen, and F. Blaabjerg, "Flicker study on variable speed wind turbines with doubly fed induction generators," *IEEE Trans. Energy Convers.*, Vol. 40, No. 4, pp. 896-905, 2005.
[3] *PSCAD User's Guide*, Manitoba HVDC Research Centre Inc., Winnipeg, MB, 2003.
[4] *EMTDC User's Guide*, Manitoba HVDC Research Centre Inc., Winnipeg, MB, 2003.
[5] R. Pena J. C. Clare, and G. M. Asher, "Doubly fed induction generator using back-to-back PWM converters and its application to variable-speed wind-energy generation," *in Proc. of Inst. Elect. Eng., Elect. Power Appl.*, Vol. 143, No. 3, pp. 231-241, 1996.
[6] A. Gole, *Vector controlled doubly fed induction generator for wind applications*, University of Manitoba, Unpublished.
[7] R. S. Pena, R. J. Cardenas, J. C. Clare, and G. M. Asher, "Control strategies for voltage control of a boost type PWM converter," *32nd Annual Power Electronics Specialists Conference*, Vol. 2, pp. 730-735, 2001.
[8] B. H. Chowdhury and S. Chellapilla, "Double-fed induction generator control for variable speed wind power generation," *Electric Power Systems Research.*, Vol.76, pp. 786-800, 2006.
[9] J. Arrillaga, N. R. Watson, and S. Chen, *Power System Quality Assessment*. West Sussex, England: JohnWiley & Sons, 2000.
[10] *Electromagnetic Compatibility (EMC)-Part 4: Testing and Measurement Techniques-Section 15: Flicker meter-Functional and Design Specifications*, IEC Std. 61 000-4-15, Nov. 1997.
[11] A. Tapia, G. Tapia, J. X. Ostolaza and J. R. Saenz, "Modeling and control of a wind turbine driven doubly fed induction generator," *IEEE Trans. Energy Convers.*, Vol.18, No. 2, pp. 194-204, 2003.

Yun-Seong Kim was born in Korea on May 26, 1982. Currently, he is a MS Student in the School of Electrical Engineering at INHA University, Incheon. His research interests include WT, distributed generation, and microgrids.

Aditya Marathe was born in India, on January 4, 1985. He graduated from the Indian Institute of Technology, Kharagpur, India with a Bachelor degree in Electrical Engineering. His research interests include power generation, renewable energy, energy efficiency and electric vehicles

Dong-Jun Won (M' 2005) was born in Korea, on January 1, 1975. He received his B.S, M.S., and Ph.D. degrees in Electrical Engineering from Seoul National University, Seoul, Korea in 1998, 2000, and 2004, respectively. He was a Postdoctoral Fellow with the APT Center, University of Washington, Seattle. Currently, he is an assistant professor with the School of Electrical Engineering at INHA University, Incheon, Korea. His research interests include power quality, dispersed generation, renewable energy, and hydrogen economy.